IEEE Photonics Journal
An IEEE Photonics Society Publication

Open Access

Experimental Investigation on Improved Predistortion Circuit for Directly Modulated Radio Over Fiber System

Volume 9, Number 5, October 2017

Shichao Chen
Lei Deng
Yao Ye
Xiaoman Chen
Mengfan Cheng
Ming Tang
Songnian Fu
Fengguang Luo
Deming Liu

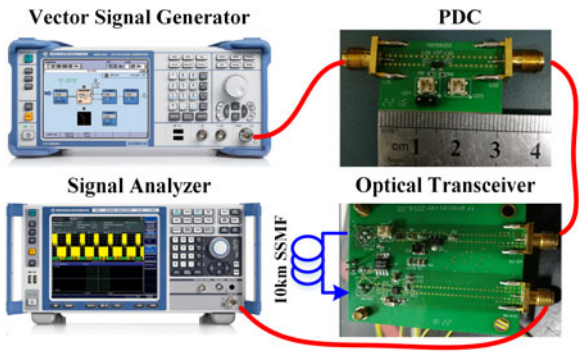

DOI: 10.1109/JPHOT.2017.2727687
1943-0655 © 2017 IEEE

IEEE photonics SOCIETY

IEEE

Experimental Investigation on Improved Predistortion Circuit for Directly Modulated Radio Over Fiber System

Shichao Chen,[1] Lei Deng,[1] Yao Ye,[2] Xiaoman Chen,[1] Mengfan Cheng,[1] Ming Tang,[1] Songnian Fu,[1] Fengguang Luo,[1] and Deming Liu[1]

[1]Next Generation Internet Access National Engineering Laboratory (NGIA), School of Optical and Electronic Information, Huazhong University of Science and Technology (HUST), Wuhan 430074, China
[2]School of Electronic Information and Communications, Huazhong University of Science and Technology (HUST), Wuhan 430074, China.

DOI:10.1109/JPHOT.2017.2727687

Manuscript received June 6, 2017; revised July 2, 2017; accepted July 12, 2017. Date of publication July 20, 2017; date of current version July 25, 2017. This work was supported in part by the National "863" Program of China under Grant 2015AA016904, in part by the National Nature Science Foundation of China under Grants 61675083, 61331010, 61505061, and 61471179, and in part by the Fundamental Research Funds for the Central Universities HUST under Grant 2017KFKJXX010. Corresponding author: Lei Deng (e-mail: denglei_hust@mail.hust.edu.cn)

Abstract: An extension of the conventional dual Schottky diode-based predistortion circuit (PDC) is proposed to linearize directly modulated radio over fiber (RoF) system. The main advantages of the proposed PDC are simple configuration, excellent distortion suppression, and broad bandwidth from dc to 6 GHz. By using the proposed cascaded Schottky diodes-based PDC, the condition of third-order intermodulation nonlinearities suppression can be more easily satisfied and the optimal linearization effect can be achieved due to the fact that it has more circuit adjustment parameters. The experimental results show that by using the proposed PDC, the spurious-free dynamic range (SFDR) @2 GHz of the optical transceiver which is designed by ourselves can be improved from 93.8 dB·Hz$^{2/3}$ to 112.1 dB·Hz$^{4/5}$ in a 1-Hz bandwidth, corresponding to 7.21% error vector magnitude performance improvement for 20 MHz 64QAM-OFDM @2 GHz signal transmission over 10 km standard single mode fiber. The linearity improvement by using the proposed PDC has also been verified in a commercial optical transceiver based RoF system, and the achieved SFDR @ 2 GHz can be increased from 102.8 dB·Hz$^{2/3}$ to 121.6 dB·Hz$^{4/5}$ in a 1-Hz bandwidth.

Index Terms: Radio over fiber (RoF), fiber optics link and subsystems, microwave photonics.

1. Introduction

To support the booming mobile data caused by the huge amounts of mobile applications, the 5th generation (5G) mobile communication network is widely expected since it offers more than 1000 times the capacity than current cellular system [1]. Owing to the cost-effective implementation, radio over fiber (RoF) technology has attracted great attention in 5G cellular system [2]. There are two types of RoF systems: directly-modulated and externally-modulated RoF systems. The RoF system based on directly-modulated distributed feedback (DFB) laser is preferred due to its extremely low cost and simplified configuration compared with externally-modulated RoF systems using electro-absorption modulator (EAM) and Mach-Zehnder modulator (MZM) [3]–[5]. However,

the transmission performance of directly-modulated RoF systems is mainly affected by the nonlinear intermodulation distortions which are generated by optical and electrical components, especially directly-modulated DFB lasers [6]. Among all the nonlinear intermodulation distortions, the third-order intermodulation distortion (IMD3) components are predominant and not easy to be filtered out due to their proximity with the desired signals [7].

To suppress the IMD3, various linearization approaches have been investigated [8]–[18]. Generally, additional devices are used to produce new nonlinearities that have equal amplitude but anti-phase with the nonlinear items for IMD3 suppression. For example, the optical feed-forward compensation in [8] can not only suppress the IMD3 but also reduce the laser intensity noise. This scheme involves two pairs of commercial laser diode and photodiode, and the achieved spurious free dynamic range (SFDR) is 107 dB·Hz$^{2/3}$ with the limited bandwidth of 500 MHz. Moreover, the feed-forward linearization scheme requires much concern about optical-coupling ratio and the effect of loop imbalance to realize optimal IMD3 suppression [9], leading to the increased system complexity. To simplify the system structure, digital signal post-compensation schemes have been demonstrated in [10]–[12] to suppress IMD3 effectively at the expense of expensive analog to digital converter and digital to analog converter, and SFDR of 120 dB·Hz$^{2/3}$ over a 6 GHz electrical signal bandwidth is achieved for a standard $LiNbO_3$ MZM-based RoF system in [12]. Due to the fact that Schottky barrier diode (SBD) has opposite nonlinear characteristics [13], SBD-based pre-distortion schemes [13]–[18] are considered as pretty-good solutions for IMD3 suppression for their simple structure, low cost and ultra-bandwidth. SBD-based pre-distortion circuit is used for both directly-modulated and externally-modulated RoF systems in [17], and SFDR of 117.5 dB·Hz$^{4/5}$ in a 1-Hz bandwidth is achieved for a commercial DFB based RoF system. However, once the circuit board is fabricated, the only parameter that can be tuned is the bias current [18], and thus it's hard to satisfy the condition to eliminate the IMD3 completely. Therefore, it is highly desired to propose a linearization technique for directly-modulated RoF system which demands lower cost, broader bandwidth and more excellent linearizing performance.

In this paper, an extension of the conventional dual SBD-based pre-distortion circuit (PDC) in [18] is proposed and applied on the uncooled DFB laser-based optical transceiver, and this optical transceiver is designed by ourselves. By using the proposed PDC which is composed of cascaded SBDs, more adjustable circuit parameters can be achieved to realize broadband-bandwidth (from DC to 6 GHz) and maximum IMD3 suppression. In our experiment, the SFDR @ 2 GHz of the RoF system can be improved from 93.8 dB·Hz$^{2/3}$ to 112.1 dB·Hz$^{4/5}$ with 18.3 dB SFDR improvement in a 1-Hz bandwidth, corresponding to 7.21% error vector magnitude (EVM) performance improvement for 20 MHz 64QAM-OFDM @2 GHz signal transmission over 10 km standard single mode fiber (SSMF). Moreover, the same linearity improvement could be observed in a commercial optical transceiver-based RoF system, and the achieved SFDR value @ 2 GHz can be increased from 102.8 dB·Hz$^{2/3}$ to 121.6 dB·Hz$^{4/5}$ in a 1-Hz bandwidth. Therefore, the proposed PDC is highly suitable for directly-modulated RoF system in future 5G cellular system.

2. Operation Principle

Fig. 1 illustrates the schematic diagram of the proposed PDC and the designed optical transceiver. In the proposed PDC, there are four low-barrier-voltage type SBDs (HSMS8202) which are driven by two tuning bias voltages U_1 and U_2, as shown in Fig. 1(a). Generally, only odd order nonlinear components induced by PDC are useful for IMD3 suppression in RoF system, so these two pairs of SBDs are placed in an anti-parallel manner to avoid producing even order nonlinear components [14]. Broadband bias-tee (TCBT-14) is used to replace inductor and capacitor for integration purpose, and the thin-film resistor in series with each SBD is carefully chosen to match the characteristic impedance (typically 50Ω) of radio frequency (RF) transmission line in printed circuit board (PCB). As shown in Fig. 1(b), the designed optical transceiver is composed of low-noise amplifier, electrical bias-tee, commercial 10G-class distributed feedback (DFB) laser with wavelength of 1310 nm and photodiode (PD), trans-impedance amplifier (TIA), and power amplifier (PA).

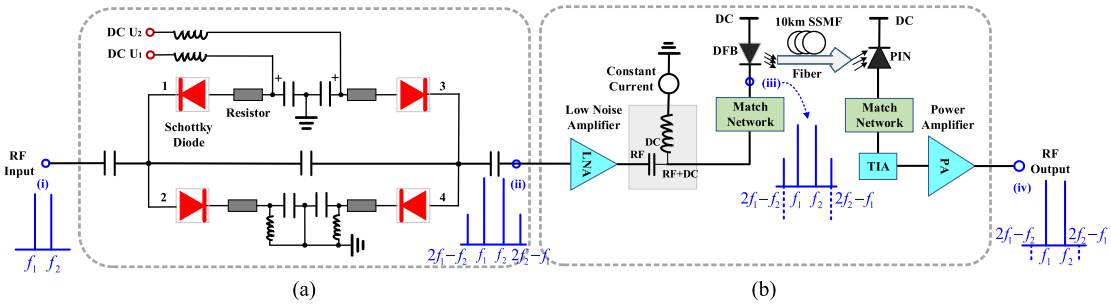

Fig. 1. Schematic diagram of the proposed pre-distortion circuit (a) and the designed optical transceiver (b).

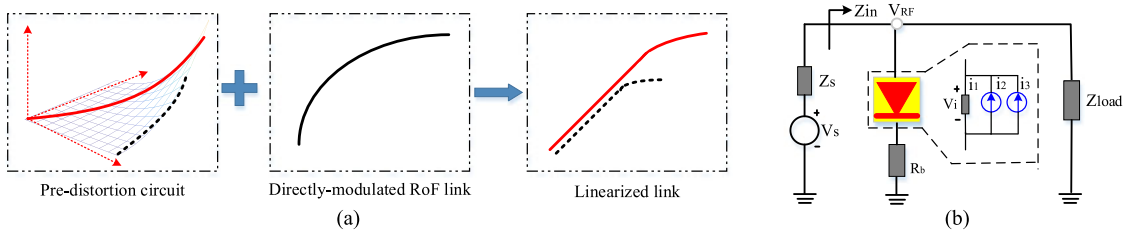

Fig. 2. Principle of linearization by using the proposed PDC (a), and the equivalent circuit of the used SBD (b).

The brief principle of linearization by using PDC can be explained by a nonlinear transfer function model, as shown in Fig. 2(a). When the transfer function of the used SBDs is exactly inversed with that of directly-modulated RoF system, the obtained transfer function will be linear. By using the proposed PDC which could be tuned by two different bias voltages, the achieved transfer function of PDC (as shown in the red and solid line in Fig. 2(a)) are more flexible than the conventional one (as shown in the black and dash line in Fig. 2(a)) which can only be controlled by one bias voltage in practice [18]. Therefore, the achieved transfer function of the proposed PDC could be easier and more accurate to match the transfer characteristic of the directly-modulated RoF system. In our scheme, by carefully adjusting these two bias voltages, the magnitude of IMD3 generated by PDC is equal to the magnitude of IMD3 induced by DFB laser and the phase difference is π, resulting in the optimal IMD3 elimination.

By using the small-signal approximation, the usual current-voltage characteristic of a SBD could be expanded into Taylor series [19], [20] and expressed as

$$i = I_S e^{V_b q/(kT)} + \sum_{n=1}^{\infty} g_n v^n \tag{1}$$

where V_b and v denote the static bias-voltage and the dynamic small-signal which are driven on SBD respectively. I_S represents the saturation current, and g_n can be described as

$$g_n = I_S(q/(kT))^n e^{V_b q/(kT)}/n!, \tag{2}$$

where q, k and T are the elementary charge constant, Boltzmann constant and working temperature, respectively.

After the first part of PDC which is composed of the first and second SBD as shown in Fig. 1, the output signal V_{RF1} can be expressed as

$$V_{RF1} = \beta_1 V_{RF} + \beta_3 {V_{RF}}^3, \tag{3}$$

where V_{RF} is the input RF signal. Even order nonlinear components are completely suppressed due to the use of push-pull structure, and higher order nonlinearities are ignored due to their negligible contribution to nonlinear distortions. The nonlinearity coefficient β_1 and β_3 can be derived

using the equivalent model as shown in Fig. 2(b). According to the nonlinear model described in [19], [20], the equivalent circuit of SBD can be replaced by one linear conductor and several current sources, and the nonlinear conductor can be substituted with a conductor g_1 and nonlinear current source i_2 and i_3. Obviously,

$$\begin{aligned} i_1 &= g_1 V_1 \\ i_2 &= g_2 V_1^2 \\ i_3 &= 2g_2 V_1 V_2 + g_3 V_1^3 \end{aligned} \tag{4}$$

where V_1 and V_2 represent the voltage applied to the conductance g_1 due to current sources i_1 and i_2, respectively. By using circuit theory and utilizing (1), (2) and (4), β_1 and β_3 can be given by

$$\begin{aligned} \beta_1 &= \frac{(1 + g_1 R_b) Z_{load}}{(1 + g_1 R_b)(Z_S + Z_{load}) + g_1 Z_S Z_{load}} \\ \beta_3 &= \frac{\left[2g_2^2 (Z_S Z_{load} + R_b (Z_S + Z_{load})) + g_3\right] Z_S Z_{load}^4}{((1 + g_1 R_b)(Z_S + Z_{load}) + g_1 Z_S Z_{load})^4} \end{aligned} \tag{5}$$

where Z_S and Z_{load} is the impedance of signal source and the load, respectively, and R_b represents thin-film resistor in series. It is noted that the transmission lines which are used for impedance matching in this circuit are neglected for simplicity in our analysis.

In the proposed PDC, the relationship between the tuning voltage U and the static bias-voltage V_b can be described as

$$U = 2(V_b + i \cdot R_b) \approx 2V_b + 2I_S R_b e^{V_b q/(kT)} \tag{6}$$

Due to the fact that the series resistance R_b is fixed once PDC is fabricated, β_1 and β_3 can be simplified and rewritten as a function of the first tuning voltage U_1 according to (2) and (5), (6). Assuming $\beta_1 = f(U_1)$ and $\beta_3 = h(U_1)$, (3) can be rewritten as

$$V_{RF1} = f(U_1) V_{RF} + h(U_1) {V_{RF}}^3 \tag{7}$$

Similarly, the output signal V_{RF2} of the second part of the proposed PDC which is composed of the third and fourth SBD as shown in Fig. 1 can be expressed as

$$V_{RF2} = f(U_2) V_{RF1} + h(U_2) {V_{RF1}}^3, \tag{8}$$

where U_2 is the tuning voltage in these two SBDs. Substituting (7) to (8), (8) can be rewritten as

$$V_{RF2} = f(U_2) f(U_1) V_{RF} + \left(f(U_2) h(U_1) + h(U_2) f^3(U_1)\right) {V_{RF}}^3 \tag{9}$$

Generally, by ignoring distortions higher than 3rd order due to their negligible contribution, the output signal of a directly-modulated RoF system could be given by $V_{out} = \gamma_1 V_{in} + \gamma_2 {V_{in}}^2 + \gamma_3 {V_{in}}^3$, where γ_1, γ_2 and γ_3 are the nonlinearity coefficients. Based on the above analysis, when the proposed PDC scheme is adopted, the output signal of RoF system can be rewritten as

$$\begin{aligned} V_{out} = {} & \gamma_1 f(U_2) f(U_1) V_{in} + \gamma_2 f^2(U_2) f^2(U_1) {V_{in}}^2 \\ & + \left(\gamma_1 f(U_2) h(U_1) + \gamma_1 h(U_2) f^3(U_1)\right. \\ & \left. + \gamma_3 f^3(U_2) f^3(U_1)\right) {V_{in}}^3 \end{aligned} \tag{10}$$

Obviously, to completely suppress IMD3, the following condition must be satisfied,

$$\gamma_1 f(U_2) h(U_1) + \gamma_1 h(U_2) f^3(U_1) + \gamma_3 f^3(U_2) f^3(U_1) = 0 \tag{11}$$

It could be clearly observed that if $h(U_1) = 0$, (11) can be simplified as

$$\gamma_1 h(U_2) + \gamma_3 f^3(U_2) = 0 \tag{12}$$

In this case, only U_2 is needed to be tuned for IMD3 elimination, and the proposed scheme is simplified down to a dual SBD-based PDC as same as the scheme reported in [18]. In this dual

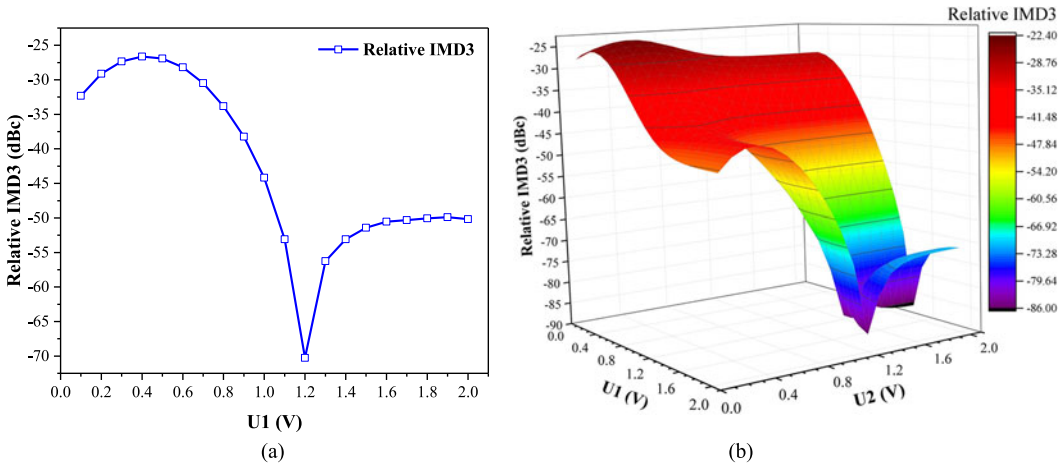

Fig. 3. Simulation curves of relative IMD3 versus bias voltages in RoF system by using the dual SBD-based PDC in [18] (a) and the proposed PDC (b).

SBD-based PDC scheme, it is not easy to make $\gamma_1 h(U_2) + \gamma_3 f^3(U_2)$ small enough just by tuning one bias voltage U_2 in practice. However, there are at least two adjustable circuit parameters U_1 and U_2 in the proposed PDC, and these two parameters could be used for tuning to achieve maximum IMD3 suppression.

To evaluate the feasibility of the proposed scheme, a simulation setup based on MATLAB has been built up. The simulation curves of relative IMD3 defined as IMD3 to fundamental component power ratio versus bias voltages in directly-modulated RoF system by using the dual SBD-based PDC [18] and the proposed PDC are shown in Fig. 3(a) and (b) respectively. In the simulation, a two-tone RF signal of 0 dBm is used, and the frequency is set to 1.999 GHz and 2.001 GHz. The transfer function of the proposed PDC is calculated by (3) and (5). Considering the actual experimental condition, the tuning voltage step is set to 0.1 V. As shown in Fig. 3(a), the relative IMD3 could be decreased to -70.4 dBc when $U_1 = 1.2\,V$, and relative IMD3 value is sensitive to bias voltage when close to the best IMD3 elimination point, making it not easy to suppress IMD3 completely in practice. However, by using the proposed scheme, the achieved relative IMD3 is -86.8 dBc when $U_1 = 1.5$ V and $U_2 = 1.7\,V$. Moreover, the measured relative IMD3 value is below -80 dBc and it changes slowly when U_1 and U_2 vary around 1.5 V and 1.7 V respectively, resulting in the increase of bias voltage margin.

3. Experimental Setup and Results

The experimental setup of a RoF system by using the proposed PDC and optical transceiver designed by ourselves are shown in Fig. 4, and 10 km SSMF is used in the test. The dual SBD-based PDC reported in [18] is also designed and fabricated for comparison in our experiment. The size of the proposed PDC and optical transceiver is 30 mm$\times$17 mm and 65 mm$\times$45 mm respectively. By using a vector network analyzer (VNA, R&S ZVL6), the S-parameters of the proposed PDC and optical transceiver are measured. As shown in Fig. 5(a) and (b), the results indicate that the effective bandwidth of optical transceiver is from 0.5 GHz to 6 GHz, and this high-pass filtering property could be attributed to the used high power amplifier. The designed PDC can cover from DC to 6 GHz, and the measured S21 value is decreased to -3 dB until 6 GHz.

In our test, a two-tone input RF signal is generated by a vector signal generator (VSG, R&S SMBV100A). The RF power is set to 0 dBm, and the frequency is set to 1.999 GHz and 2.001 GHz. An electrical signal analyzer (ESA, R&S FSV) is used to measure power of the nonlinearities, including the third-order intermodulation distortion and the fifth-order intermodulation distortion (IMD5). The same optical transceiver is used for both the dual SBD-based PDC and the proposed

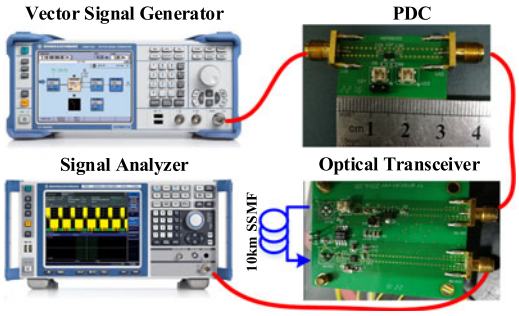

Fig. 4. Experimental setup of a RoF system by using the proposed PDC and optical transceiver designed by ourselves.

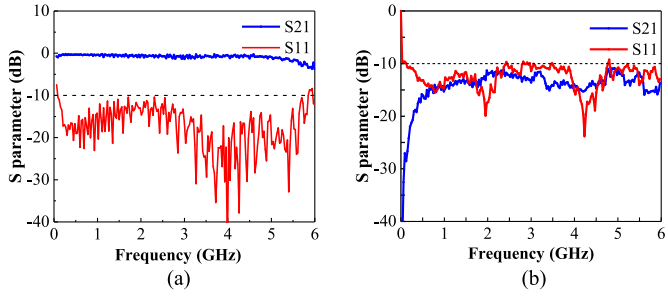

Fig. 5. Measured S-parameters of the proposed PDC (a) and optical transceiver (b).

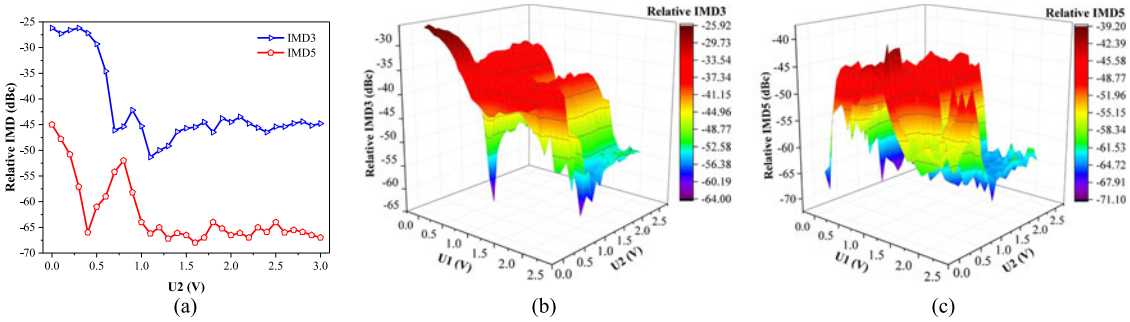

Fig. 6. Measured relative IMD3 and IMD5 versus bias voltages in RoF system with the dual SBD-based PDC (a) and the proposed PDC (b) and (c).

PDC. Note that relative IMD3/IMD5 defined as IMD3/IMD5 to fundamental component power ratio are adopted in Fig. 6 to get rid of the influence induced by the changes of fundamental component. Fig. 6(a) shows the measured relative IMD3 and IMD5 as a function of different bias voltage U_2 in the dual SBD-based PDC. Fig. 6(b) and (c) illustrate the measured relative IMD3 and IMD5 as a function of different two bias voltages U_1 and U_2 in the proposed PDC respectively. It could be clearly observed that in the RoF system where the dual SBD-based PDC is used, the relative IMD3 and IMD5 can be decreased to -51.1 dBc and -63.5 dBc respectively when $U_2 = 1.1\,V$. However, by using the proposed PDC, the relative IMD3 and IMD5 can be further decreased to -63.2 dBc and -62.7 dBc respectively when $U_1 = 2.0\,V$ and $U_2 = 1.1\,V$, as shown in Fig. 6(b) and (c). Obviously, this RoF system is now limited by IMD5. It should be noted that relative IMD3 and IMD5 could not reach the minimum value simultaneously, so the linearization effect of the RoF system is required to be optimized by considering both IMD3 and IMD5. As last, the bias voltages of $U_1 = 2.0\,V$ and $U_2 = 1.1\,V$ are chosen for EVM performance evaluation in our experiment.

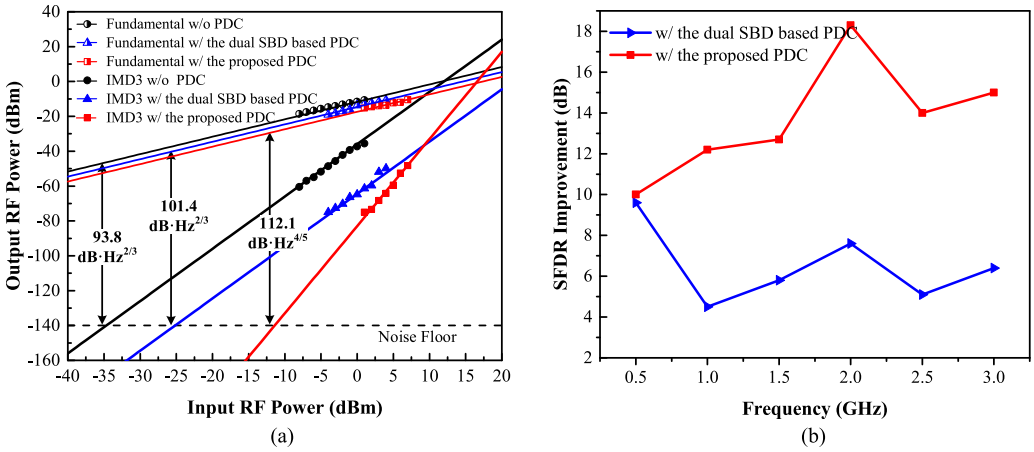

Fig. 7. Measured SFDR (a) and SFDR improvements (b) in our optical transceiver based RoF system with the proposed PDC and the dual SBD-based PDC.

Fig. 7(a) shows the measured output RF power with respect to input RF power and the calculated SFDR of the RoF system without PDC, with the proposed PDC and with the dual SBD-based PDC, respectively. In the test, the central frequency and frequency spacing of two-tone RF signal are set to 2 GHz and 2 MHz, respectively. It could be clearly observed that the SFDR is improved from 93.8 dB·Hz$^{2/3}$ to 101.4 dB·Hz$^{2/3}$, corresponding to 7.6 dB SFDR improvement in a 1-Hz bandwidth due to the use of dual SBD-based PDC. The SFDR is limited by IMD3, yielding a slope-of-3 dependence on input RF power. The noise floor in our test is −140 dBm/Hz. However, by using the proposed PDC, two bias voltages could be tuned in turn to maximum the IMD3 suppression, and the results show that 18.3 dB SFDR improvement from 93.8 dB·Hz$^{2/3}$ to 112.1 dB·Hz$^{4/5}$ in a 1-Hz bandwidth is achieved. It means that the power of residual IMD3 components is smaller than that of residual IMD5 components, and this RoF system is now limited by IMD5, yielding a slope-of-5 dependence on input RF power. The SFDR improvements by using a two-tone RF signal with different central frequency from 0.5 GHz to 3 GHz are also tested and shown in Fig. 7(b). Overall, the SFDR improvements fluctuate over the bandwidth, and the maximum SFDR improvement of 18.3 dB (1-Hz instantaneous bandwidth) is obtained when the central frequency of two-tone RF signal is 2 GHz. However, the proposed PDC obviously outperforms the dual SBD-based PDC over the test bandwidth.

The propose PDC and optical transceiver are also evaluated by 20 MHz 64QAM-OFDM signal with carrier frequency of 2 GHz, and 10km SSMF is used in our test. In the experiment, 20 MHz 64QAM-OFDM signal is generated by VSG (R&S SMBV100A), and the EVM performance of the received RF signal is calculated by an electrical signal analyzer (ESA, R&S FSV). Fig. 8 shows the measured EVM performance of the RoF system without PDC, with the proposed PDC and with the dual SBD-based PDC respectively. The EVM performance is calculated as a function of the input RF power of the optical transceiver considering that the insertion loss of PDC is around 2 dB. In the RoF system without PDC, the achieved output RF power is −3 dBm at the EVM limit of 8%. By using the dual SBD-based PDC, the achieved output RF power can be increased to −1 dBm at the EVM limit. However, by using the proposed PDC the achieved maximum input RF power can be increased to 1 dBm notably at the EVM limit. The constellation diagrams of the received RF signals are also plotted in the insets of Fig. 8. It could be clearly observed that without PDC, the calculated EVM is 9.18% when the input RF power of optical transceiver is −2 dBm. By using the dual SBD-based PDC, the EVM value is decreased to 5.22%, but the EVM value could be further reduced to 1.97% if the proposed PDC is used. Obviously, the proposed PDC has better linearization effect with 18.3 dB SFDR and 7.21% EVM performance improvement.

To verify the applicability and generality of the proposed PDC, experimental investigations are performed in another RoF system based on the commercial directly-modulated transmitter and

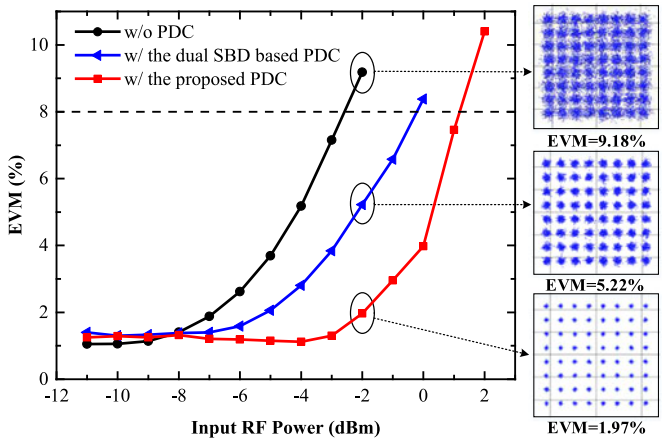

Fig. 8. Measured EVM performance in our optical transceiver based RoF system without PDC, with the proposed PDC and with the dual SBD-based PDC.

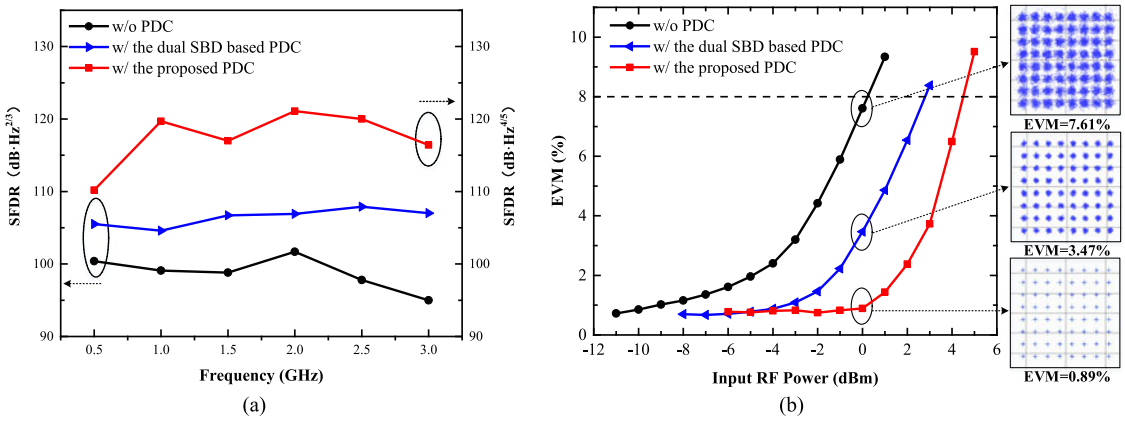

Fig. 9. Measured SFDR (a) and EVM performance (b) in commercial transceiver based RoF system without PDC, with the proposed PDC and with the dual SBD-based PDC.

receiver (FT-0XN310FS-V000 and FR-0XB00FS-V000 made by SKYASTAR), and the dual SBD-based PDC is also tested for comparison. As shown in Fig. 9(a), the SFDR with respect to frequency of this commercial transceiver can reach up to 102.8 dB·Hz$^{2/3}$ (in a 1-Hz bandwidth) at 2 GHz. The dual SBD-based PDC could help to increase SFDR value to 107.3 dB·Hz$^{2/3}$ (in a 1-Hz bandwidth) at 2 GHz, and the maximum SFDR value of 121.6 dB·Hz$^{4/5}$ can be achieved by using the proposed PDC. In this case, this RoF system is limited by IMD5. Similarly, 20 MHz 64QAM-OFDM signal with carrier frequency of 2 GHz is transmitted over 10 km SSMF for EVM performance testing. Obviously, at a given input RF power 0 dBm, the calculated EVM value is 7.61%, 3.47%, and 0.89% without PDC, with the dual SBD-based PDC and with the proposed PDC respectively, as shown in Fig. 9(b). The constellations of the received RF signals are also plotted in the insets of Fig. 9(b). Overall, the proposed PDC proves to be more effective for linearizing commercial optical transceiver.

5. Conclusion

In conclusion, we have successfully demonstrated an improved pre-distortion circuit for directly-modulated radio over fiber system. By using the proposed cascaded Schottky diodes based PDC, the tuning dimension is increased and the maximum IMD3 could be easily achieved. The experimental results show that the SFDR can be improved to 112.1 dB·Hz$^{4/5}$ with 18.3 dB improvement (in a 1-Hz instantaneous bandwidth) in the RoF system using optical transceiver designed by

ourselves. At a given input RF power of −2 dBm, the proposed PDC can help to increase the EVM performance of 20 MHz 64QAM-OFDM signal from 9.18% to 1.97%. The proposed PDC also proves to be effective for commercial optical transceiver, whose SFDR can be extremely improved to 121.6 dB·Hz$^{4/5}$. These results indicate that the proposed PDC performs well in linearizing the directly-modulated RoF system. Since the proposed PDC has the advantages of simple configuration, excellent distortion suppression and broad bandwidth from DC to 6GHz, the proposed scheme has great potential applications for directly-modulated RoF system in future 5G cellular system.

References

[1] J. G. Andrews *et al.*, "What will 5G be," *IEEE J. Sel. Areas Commun.*, vol. 32, no. 6, pp. 1065–1082, Jun. 2014.
[2] B. Lannoo, D. Colle, M. Pickavet, and P. Demeester, "Radio-over-fiber-based solution to provide broadband internet access to train passengers [Topics in optical communications]," *IEEE Commun. Mag.*, vol. 45, no. 2, pp. 56–62, Feb. 2007.
[3] D. Wake, A. Nkansah, and N. J. Gomes, "Radio over fiber link design for next generation wireless systems," *J. Lightw. Technol.*, vol. 28, no. 16, pp. 2456–2464, Aug. 2010.
[4] Y. Ye *et al.*, "Simultaneous suppression of even-order and third-order distortions in directly-modulated analog photonic links," *IEEE Photon. J.*, vol. 9, no. 3, pp. 1–12, Jun. 2017.
[5] B. G. Kim, S. H. Bae, H. Kim, and Y. C. Chung, "DSP-based CSO cancellation technique for RoF transmission system implemented by using directly modulated laser," *Opt. Express*, vol. 25, no. 11, pp. 12152–12160, May 2017.
[6] J. H. Winters and R. D. Gitlin, "Electrical signal processing techniques in long-haul fiber-optic systems," *IEEE Trans. Commun.*, vol. 38, no. 9, pp. 1439–1453, Sep. 1990.
[7] K. Xu *et al.*, "Microwave photonics: Radio-over-fiber links, systems, and applications [Invited]," *Photon. Res.*, vol. 2, no. 4, pp. B54–B63, Aug. 2014.
[8] Y. T. Moon, J. W. Jang, W. K. Choi, and Y. W. Choi, "Simultaneous noise and distortion reduction of a broadband optical feedforward transmitter for multi-service operation in radio-over-fiber systems," *Opt. Express*, vol. 15, no. 19, pp. 12167–12173, Sep. 2007.
[9] T. Ismail, C. P. Liu, J. E. Mitchell, and A. J. Seeds, "High-dynamic-range wireless-over-fiber link using feedforward linearization," *J. Lightw. Technol.,* vol. 25, no. 11, pp. 3274–3282, Nov. 2007.
[10] Y. Ye *et al.*, "A broadband and high linearity directly-modulated analog photonic link based on push-pull structure and digital signal post-compensation," in *Proc. Opt. Fiber Commun. Conf.*, Mar. 2016, Paper TH2A.22.
[11] A. Fard, S. Gupta, and B. Jalali, "Digital broadband linearization technique and its application to photonic time-stretch analog-to-digital converter," *Opt. Lett.*, vol. 36, no. 7, pp. 1077–1079, Apr. 2011.
[12] D. Lam, A. M. Fard, B. Buckley, and B. Jalali, "Digital broadband linearization of optical links," *Opt. Lett.*, vol. 38, no. 4, pp. 446–448, Feb. 2013.
[13] L. Roselli *et al.*, "Analog laser predistortion for multiservice radio-over-fiber systems," *J. Lightw. Technol.*, vol. 21, no. 5, pp. 1211–1223, May 2003.
[14] G. C. Wilson *et al.*, "Predistortion of electroabsorption modulators for analog CATV systems at 1.55 um," *J. Lightw. Technol.*, vol. 15, no. 9, pp. 1654–1662, Sep. 1997.
[15] H. Son, K. J. Kim, Y. Li, C. I. Park, and Y. W. Choi, "Simple electrical predistortion method using schottky diode for radio-over-fiber systems," *IEEE Photon. Technol. Lett.*, vol. 27, no. 8, pp. 907–910, Apr. 2015.
[16] C. Han, S. H. Cho, H. S. Chung, and J. H. Lee, "Linearity improvement of directly-modulated multi-IF-over-fibre LTE-A mobile fronthaul link using shunt diode predistorter," in *Proc. Opt. Comm. Eur. Conf.*, Sep. 2015, pp. 1–3.
[17] R. Zhu, X. Zhang, D. Shen, and Y. Zhang, "Ultra broadband predistortion circuit for radio-over-fiber transmission systems," *J. Lightw. Technol.*, vol. 34, no. 22, pp. 5137–5145, Nov. 2016.
[18] X. Zhang, S. Saha, R. Zhu, T. Liu, and D. Shen, "Analog pre-distortion circuit for radio over fiber transmission," *IEEE Photon. Technol. Lett.*, vol. 28, no. 22, pp. 2541–2544, Nov. 2016.
[19] S. A. Maas, *Nonlinear Microwave and RF Circuits*. Norwood, MA, USA: Artech House, 2003.
[20] Y. Shen, B. Hraimel, X. Zhang, GE. Cowan, K. Wu, and T. Liu, "A novel analog broadband RF predistortion circuit to linearize electro-absorption modulators in multiband OFDM radio-over-fiber systems," *IEEE Trans. Microw. Theory Techn.*, vol. 58, no. 11, pp. 3327–3335, Nov. 2010.